International Research Journal of Innovations in Engineering and Technology (IRJIET)

ISSN (online): 2581-3048

Volume 10, Issue 5, pp 304-315, May-2026

https://doi.org/10.47001/IRJIET/2026.105041

Unified Closed-Form Load–Deflection Modeling of Spiral-Defined Telescopic Conical Compression Springs

[1]Ali Khayoun Al-Janabi, [2]Essam L. Esmail

[1,2]Department of Mechanical Engineering, College of Engineering, University of Al-Qadisiyah, Al-Diwaniyah, Iraq

E-mail: [1]ali.khayoun.mh@qu.edu.iq, [2]essam.esmail@qu.edu.iq

Abstract **- The nonlinear load-deflection response of telescopic conical compression springs is due to the gradual stacking of the coils and the change of the diameter along the spring axis. The classical theory for cylindrical springs is well established, but analytical treatments for spiral-defined conical springs are fragmented and often based on incremental coil-by-coil approaches that may lead to more inaccuracies in the prediction of their load-deflection response than the more comprehensive approaches proposed in this paper. A unified closed-form theoretical framework is presented in this paper for the load-deflection and stiffness behaviour of telescopic conical springs, whose coil centrelines follow Archimedean, logarithmic and parabolic spiral laws. The elastic deflection is determined exactly by a continuous turn-index formulation. A load-radius boundary mapping models the progressive stacking regime explicitly. Closed-form expressions are obtained for the linear and stacking regimes, the transition and collapse loads and the evolution of instantaneous stiffness. We formally prove the mathematical continuity, monotonicity, and limit correctness. By means of comparative analysis we reveal a consistent stiffness hierarchy between spiral types and the geometric mechanisms governing nonlinear response. The framework avoids incremental summation methods and offers design-ready analytical expressions, which are appropriate for optimization and parametric synthesis of nonlinear conical springs.**

Keywords: Conical compression spring, spiral geometry, nonlinear stiffness, telescopic spring, closed-form model, stacking regime, analytical mechanics.

I. INTRODUCTION

Helical compression springs are one of the most common types of elastic elements in systems of mechanical engineering, performing important functions of energy storage, load control, vibration isolation, and motion control. Classical spring theory has been extensively developed for cylindrical helical springs with a constant mean coil diameter and uniform pitch, for which well-established closed-form relationships predict linear load-deflection behaviour. However, the constraints of compactness, custom nonlinear stiffness, progressive loading and reduced solid height have led to the development of non-cylindrical spring geometries, especially conical compression springs. These springs have a coil diameter that varies along the axis and may telescope under compression so that the coils can successively nest and yield a strongly nonlinear mechanical response. Now, in the case when progressive stiffness and controlled force increase are necessary, conical compression springs are used in compact mechanisms, protective devices, actuators, suspension subsystems and precision instruments. The theory of conical springs is much less developed than the theory of cylindrical springs, although of great practical importance. Most of the existing methods are based on coil-by-coil summation or incremental numerical methods that approximate the nonlinear response by summing local compliance contributions. Such techniques are useful in practice but not analytically continuous; they are difficult to invert for design synthesis and inefficient for optimisation and parametric studies, which limits their applicability in developing more advanced spring designs and understanding their mechanical behaviour. Recent geometric modelling methods based on mathematically defined spiral centerlines (including Archimedean, logarithmic, and parabolic spiral laws) allow for the systematic control of coil radius variation and stiffness evolution, but their mechanical behaviour is not yet fully unified into a closed-form theoretical framework. The scientific and engineering problem solved in this paper is the lack of a unified closed-form regime-continuous analytical model of the load-deflection and stiffness behaviour of telescopic conical compression springs with general spiral radius laws. Current models are often limited to certain geometries, ranges of deformation or incremental formulations where transitions between regimes are masked and analytical insight is limited. In particular, the progressive stacking phase, where the coils are in contact one after another, with the number of active turns decreasing with increasing load, is often treated with stepwise or numerical methods rather than with explicit analytical expressions. The research gap is thus the absence of a continuous, closed-form theoretical formulation which (i) encompasses the spiral-defined conical springs within a unified framework that (ii) gives explicit load-deflection relationships in the linear and stacking regions,

ISSN (online): 2581-3048
Volume 10, Issue 5, pp 304-315, May-2026
https://doi.org/10.47001/IRJIET/2026.105041

(iii) provides analytical conditions for transition and collapse, and (iv) gives the stiffness evolution and comparative behaviour for different spiral laws. Such a general formulation would replace the incremental summation over the coils by expressions based on integrals, guarantee mathematical continuity between phases of deformation, and allow a parametric control orientated to design. The present paper covers this gap by proposing a unified closed-form analytical framework for telescopic conical compression springs whose coil centrelines follow the laws of Archimedean, logarithmic and parabolic spirals. The research has the following specific objectives:

- To develop a continuous turn index geometric model for spiral-defined conical springs.
- To obtain closed form load-deflection relations for the fully free (linear) regime for each type of spiral.
- To develop a general analytical formulation of the stacking regime based on the load-dependent free boundary radius.
- To obtain explicit stacking equations in closed form for Archimedean, logarithmic and parabolic spirals.
- To obtain analytical expressions for transition load, collapse load and instantaneous stiffness.
- Check for mathematical continuity, monotonicity and correct limiting behaviour across regimes.
- To establish a theoretical hierarchy of stiffnesses and comparative behaviour for spiral laws.

The following research questions guide the study:

- Can the nonlinear load-deflection response of spiral-defined telescopic conical springs in both free and stacking regimes be expressed in fully closed analytical form?
- How does the spiral radius law affect the evolution of the stiffness and the nonlinear response?
- Are the resulting closed-form models continuous and meet physical limit conditions at regime boundaries?

The research is limited to the theoretical, quasi-static, torsionally dominated analysis of telescopic conical compression springs with spirally defined coil centre lines. The formulation is based on linear elastic material behaviour, small pitch angles and purely axial loading. The contact between coils is not described in detail but is governed by the geometrical conditions of stacking. The present work does not take into account the dynamic effects of fatigue behaviour, frictional contact mechanics, local stresses, or manufacturing tolerances, which are left for future studies.

II. LITERATURE REVIEW

2.1 Scope and Objective of the Literature Review

The principles of helical compression springs have been studied for many years, and the behaviour of cylindrical springs is now well described by the established theory [1, 2]. However, non-cylindrical configurations, in particular telescopic conical springs defined by continuous spiral laws, have been less considered in the closed-form analytical modelling [3, 4], which limits the understanding of their mechanical properties and potential applications in engineering design. The present review aims at giving an overview of the main approaches to the analysis of conical and variable-radius springs, with special attention to the basic assumptions and mathematical structures. Instead of a purely descriptive summary, the emphasis is on the strengths and limitations of current approaches and on clarifying where current formulations fall short. The expressions obtained for cylindrical springs show that the axial deflection is linearly proportional to the load applied. Also geometric and material parameters are important, increasing with the third power of the mean coil radius and decreasing with the shear modulus and the fourth power of the wire diameter [2, 5]. This model was built on the elasticity theory and further reinforced by energy techniques and Castigliano variety methods, which would be eigenstate equations of spring compliance relative to the strain energy stored in torsion [6]. These simple classical equations give good estimates for linear load-deflection relations and constant stiffness expressions for cylindrical springs with coil radius and pitch constant along the axis. The success of the classical theory of springs is therefore mainly due to geometry. For conical and other non-cylindrical springs, the stiffness is not constant in the space and has to be integrated over the active length because the mean coil radius changes along the spring axis [6]. While the classical formulae are still valid locally, they do not offer any more global closed-form solutions, which restricts their use in engineering designs requiring accurate predictions of the behaviour of the springs for a variety of geometries. The first major theoretical obstacle to extending the cylindrical spring theory to geometries with variable radius is its geometric dependence. Other geometries, other than cylindrical springs, were presented to achieve design objectives difficult to reach by the most common designs, such as progressive stiffness and reduced solid height [1; 7]. Of these, conical compression springs are particularly important as they can telescope when compressed, allowing the coils to nest one after another and thus providing a compact collapse length with non-linear load build-up [4]. The usual way to characterise conical springs is to apply cylindrical formulas locally along coils of varying diameter. In practice, engineering manuals and design recommendations used simplified factors of adjustment or

ISSN (online): 2581-3048
Volume 10, Issue 5, pp 304-315, May-2026
https://doi.org/10.47001/IRJIET/2026.105041

piecewise approximations using linear variation with respect to diameter [4]. These methods were useful for engineering estimates but did not lead to continuous global analytical models in a computational sense. Later theoretical improvements include more advanced formulations and alternate compliance models for variable-geometry springs, including large deflection analyses, lateral stiffness, and full stability behaviour [6; 8]. These advances improved the level of analysis, but most still rely on segmentation or numerical integration rather than true closed-form expressions. In many works the conical spring is considered a special case of cylindrical spring, which is not quite suitable for the case when the radius changes continuously along the spring. Consequently, the resulting models are often approximate and do not correctly describe the non-linear load-deflection behaviour over the whole stacking range. One of the most common methods is coil by coil. In this method, the spring is analysed as a cylindrical one with its own radius. The spring is divided into individual coils. At a given load, only those coils that have not yet been touched are considered active. The total deflection is the sum of the contributions from the coils. As load increases, contact is made and the coils are gradually removed from the active set. The primary reason for the popularity of this method is its simplicity and the fact that it can be implemented without much difficulty, e.g., in spreadsheets or basic design tools. Often it yields reasonable results from an engineering point of view. But there are some obvious disadvantages as well. The approach is not a closed-form solution, and the results are dependent on the discretisation of the spring. Moreover, the response is obtained in a piecewise way, and continuity between the different stages is not guaranteed. This complicates the optimisation or manipulation analytically [10]. Similar assumptions are made in other simplified models where the coils are considered more or less independently and contact is approximated. These models can be useful in practice, but they are not based on a single consistent theory. Such approximations can lead to discrepancies in their predictions compared to more comprehensive approaches such as finite element analysis. Finite element analysis has also been done for detailed analysis of conical and non-linear springs [11]. In such models the coil-to-coil contact, friction and local stress effects are accurately accounted for as well as geometric nonlinearity [12, 13]. Some work on reduced-order models to increase efficiency exists, especially for simplifying complex simulations but still keeping the accuracy in the prediction of the behaviour of conical and non-linear springs. But these methods are still numerical in character and are generally used for detailed analysis rather than for the construction of general analytical relationships. Numerical methods, which are techniques used to obtain approximate solutions to mathematical problems, are useful for validation and detailed stress analysis, but they do not replace analytical load-deflection relations. They are computationally intensive, have a large number of modelling parameters, and tend to provide numerical rather than explicit equations. Therefore, they are not always suitable for parametric design, optimisation or comparison of different geometries [14]. For the case of spiral-defined conical springs, a finite element analysis is better understood as a support or verification tool and not a primary modelling approach. Beyond these efforts, a smaller body of work has tried to derive closed-form models of conical springs, usually with simplifying assumptions about the geometry, such as constant pitch. These studies show that it is possible under certain conditions to obtain analytical expressions for stiffness and non-linear load-deflection behaviour using integral-based formulations [15, 3]. Some of these results have also been used in vibration analysis and optimisation problems [16, 17]. However, most of the closed-form models available are restricted to specific geometries, often assuming a simple linear variation in radius. Typically, they do not include different laws of radius growth within a single framework. Moreover, the questions of the continuity of the deformation regimes, the derivative behaviour, and the stiffness's limits are not always treated in detail. As a consequence, the present closed-form theories are somewhat fragmented. More recently, a spiral-based description has been used to define the centreline geometry of conical springs [18]. Specifically, the Archimedean, logarithmic and parabolic spirals enable the coil radius to change smoothly as a function of the turn index. Such formulations are useful in geometric modelling and CAD-based designs. They provide continuous curvature and a controlled way to define the spring profile. They also allow a direct influence on the evolution of stiffness by the choice of the distribution of radius, which can be tailored to meet specific design requirements and performance criteria in the final product [19].The majority of work on spiral-based spring geometries has focused on geometric construction or numerical evaluation rather than a complete analytical investigation. Although some spiral laws have closed-form expressions for the load–deflection behaviour, the results are usually obtained separately and not within a single consistent framework. In particular, there is still little work on closed-form descriptions of the stacking stage and stiffness evolution and direct comparison of different spiral forms. In a broader context, classical spring theory has a sound physical basis but is mostly limited to simple geometries [1]. On this basis, existing conical spring models are partially developed but are often incremental, piecewise or based on specific geometric assumptions [4]. Numerical and finite element approaches can give accurate results, but they do not lead to explicit analytical relations and thus are of less use for general design or comparison purposes [11], particularly when engineers require straightforward formulas for quick

International Research Journal of Innovations in Engineering and Technology (IRJIET)

ISSN (online): 2581-3048

Volume 10, Issue 5, pp 304-315, May-2026

https://doi.org/10.47001/IRJIET/2026.105041

assessments and optimisations in spring design. On the one hand, spiral-based descriptions offer a flexible way of defining geometry, but the mechanical treatment is still incomplete [18]. Together, these points suggest that a general analytical framework is still lacking. In particular, a formulation is needed which can accommodate different spiral radius laws, describe the initial and stacking stages as well as explicit expressions for load deflection behaviour, stiffness and transition conditions in a consistent way. To this end, a closed-form analytical model for telescopic conical compression springs defined by Archimedean, logarithmic and parabolic spirals is developed in the present work. The approach adopts a continuous turn-index formulation rather than incremental coil summation, incorporates an explicit load-radius boundary for characterising stacking, and develops closed-form relations for the stacking stage. In this sense it extends the existing theory of conical springs to a more general and unified analytical description.

III. THEORETICAL FORMULATION

3.1 Mechanical Basis and Modeling Framework

The axial action of a helical compression spring is mainly due to the torsional deformation of the wire under load. When an axial force is applied on a closely coiled spring, the dominant deformation mechanism is the twisting of the wire cross section, not the bending of the coil centreline. Direct shear and bending curvature are small relative to the torsion under the classical assumption of a closely coiled configuration and are thus omitted from the primary formulation. This assumption is common in spring mechanics and valid for small pitch angles and moderate coil curvature. The incremental axial deflection due to torsion for a coil element of mean radius r is proportional to r^3. Hence, the total axial deflection cannot be expressed by a single constant radius formula for a coil radius that varies along the spring axis. Instead, the global response is obtained by integrating the local torsional compliance over the active turns. This observation is the main theoretical motivation for the continuous formulation used in this paper. This means the spring is represented by a continuous turn index variable instead of discrete coils. Let the turn index n_acontinuously vary from the inner active coil to the outer active coil in the interval $0 \leq n \leq n_a$, where n_a is the number of active turns. The mean radius of a coil is defined as a continuous function $r(n)$ The spring is thus represented as a one-dimensional geometric field, whose mechanical response can be computed by direct integration. This eliminates the summation over the coil and enables closed-form evaluation if $r(n)$is analytically described. The material is assumed to be isotropic and linearly elastic with shear modulus G. 'd' is the wire diameter. The load is assumed to be quasi-static and only axial. The interaction between coils is modelled in a geometrical approach of stacking constraints rather than detailed contact stress analysis. Frictional effects between coils are neglected. Contact is assumed to remove turns from elastic participation without adding any compliance. These assumptions are consistent with common analytical spring models and are sufficient to obtain closed-form load-deflection relations across regimes.

3.2 Geometric Description of Spiral-Defined Conical Springs

A conical compression spring is characterized by a monotonic variation of coil radius along the axis. In the present formulation, this variation is prescribed by an explicit spiral law relating the mean radius to the turn index. The inner and outer mean radii are denoted by r_1 and r_2, respectively. The spring's overall height is L_0, with a telescopic solid height approximately $S_L \approx d$ and an active length

$$L_a = L_0 - S_L \tag{1}$$

The per-turn clearance at the centerline, which defines the onset of coil contact, is denoted by

$$\delta_s = L_a / n_a \tag{2}$$

These relations establish the geometric bounds and contact spacing that determine the onset of stacking. Figure 1 shows the parameters of the studied spiral springs.

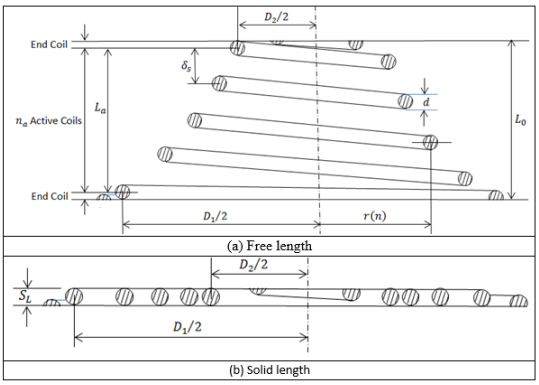

Figure 1: Parameters of the studied logarithmic spiral spring

Three spiral families are considered. For the Archimedean spiral, the radius increases linearly with the turn index. The governing relation is expressed as

$$r(n) = r_1 + \gamma n \tag{3}$$

where

$$\gamma = \frac{r_2 - r_1}{n_a} \tag{4}$$

International Research Journal of Innovations in Engineering and Technology (IRJIET)
ISSN (online): 2581-3048
Volume 10, Issue 5, pp 304-315, May-2026
https://doi.org/10.47001/IRJIET/2026.105041

is the constant rate of change of the radius per turn, r_1 and r_2 are the inner and outer radii, respectively, and n_a is the total number of turns. This form represents a linear increase of radius per turn.

For the logarithmic spiral, the radius follows an exponential law with respect to the turn index n, given by

$$r(n) = r_1 e^{kn} \tag{5}$$

where the growth constant (k) is defined as

$$k = \frac{\ln R}{n_a} \tag{6}$$

And $R = r_2/r_1$. This expression ensures that the ratio of radii between successive turns remains constant, leading to a constant ratio between successive turns.

In the parabolic spiral, the square of the radius varies linearly with the turn index according to

$$r(n)^2 = r_1^2 + \beta n \tag{7}$$

where

$$\beta = \frac{r_2^2 - r_1^2}{n_a} \tag{8}$$

Hence, the radius as a function of turn number can be written as

$$r(n) = \sqrt{r_1^2 + \beta n} \tag{9}$$

This law represents a quadratic variation of radius with turn index.

These three laws represent distinct radius-growth classes, linear, exponential, and quadratic, and therefore produce systematically different stiffness evolution. Because each law is invertible, the turn index can be expressed as a function of radius, which is essential for stacking-regime derivations.

3.3 Linear Regime Deflection: Continuous Compliance Integral

When the applied load is sufficiently small that no coils are in contact, all turns remain elastically active. This defines the linear (all-free) regime. In this regime, the total axial deflection is obtained by integrating torsional compliance along the full turn domain. Using torsion-dominated spring theory, the deflection is given by

$$\Delta = \int_0^{n_a} \frac{64\,P r(n)^3}{Gd^4}\,dn = \frac{64\,P}{Gd^4}\int_0^{n_a} r(n)^3\,dn \tag{10}$$

This equation is fundamental: it is independent of spiral type and depends only on the radius function. It establishes a universal backbone for the theory. All spiral-specific linear-regime formulas follow from evaluating this integral with the appropriate $r(n)$.

From Eq. (3) and Eq. (10), we get:

$$\Delta_{lin.Arch}(P) = \frac{64\,P}{Gd^4}\int_0^{n_a}(r_1 + \gamma n)^3\,dn \tag{11}$$

By computing the integral, we get

$$\Delta_{lin.Arch}(P) = \frac{64\,P}{Gd^4}\left[r_1^3 n + \frac{3}{2}r_1^2\gamma n^2 + r_1\gamma^2 n^3 + \frac{1}{4}\gamma^3 n^4\right]_0^{n_a} \tag{12}$$

Thus

$$\Delta_{lin.Arch}(P) = \frac{64\,P}{Gd^4}\cdot\frac{n_a(r_2^4 - r_1^4)}{4(r_2 - r_1)} \tag{13}$$

The spring rate (instantaneous stiffness) is linear

$$R_{lin.Arch} = \frac{Gd^4(r_2 - r_1)}{16\,n_a(r_2^4 - r_1^4)} \tag{14}$$

The resulting stiffness is constant and depends on a fourth-order polynomial combination of inner and outer radii.

From Eq. (5) and Eq. (10), we get:

$$\Delta_{lin.log}(P) = \frac{64\,P}{Gd^4}\int_0^{n_a} r_1^3 e^{3kn}\,dn \tag{15}$$

By computing the integral, we get

$$\Delta_{lin.log}(P) = \frac{64\,P}{Gd^4}\cdot\frac{r_1^3}{3k}(e^{3kn_a} - 1) \tag{16}$$

Using Eq. (6), Eq. (16) becomes

$$\Delta_{lin.log}(P) = \frac{64\,P}{Gd^4}\frac{(r_2^3 - r_1^3)n_a}{3\ln(r_2/r_1)} \tag{17}$$

The spring rate is

$$R_{lin.log} = \frac{3Gd^4\ln(r_2/r_1)}{64\,n_a(r_2^3 - r_1^3)} \tag{18}$$

For the parabolic, let $s(n) = r(n)$. By substituting s into Eq. (7), we have

$$s^2 = r_1^2 + \beta n \tag{19}$$

Differentiating both sides gives

$$2s\,ds = \beta\,dn \tag{20}$$

or equivalently,

$$dn = (2s/\beta)\,ds \tag{21}$$

ISSN (online): 2581-3048
Volume 10, Issue 5, pp 304-315, May-2026
https://doi.org/10.47001/IRJIET/2026.105041

From Eq. (10) and Eq. (21), we get:

$$\Delta_{lin.par}(P) = \frac{64\,P}{Gd^4}\int_{s=r_1}^{r_2} s^3\,\frac{2s}{\beta}\,ds \tag{22}$$

or

$$\Delta_{lin.par}(P) = \frac{64\,P}{Gd^4}\cdot\frac{2}{\beta}\int_{r_1}^{r_2} s^4\,ds \tag{23}$$

By computing the integral, we get

$$\Delta_{lin.par}(P) = \frac{64\,P}{Gd^4}\cdot\frac{2}{\beta}\cdot\frac{1}{5}(r_2^5 - r_1^5) \tag{24}$$

Using Eq. (8), Eq. (24) becomes

$$\Delta_{lin.par}(P) = \frac{64\,P}{Gd^4}\cdot\frac{2n_a}{5(r_2^2-r_1^2)}(r_2^5 - r_1^5) \tag{25}$$

Thus

$$\Delta_{lin.par}(P) = \frac{128 n_a\,P}{5Gd^4(r_2^2-r_1^2)}(r_2^5 - r_1^5) \tag{26}$$

And

$$R_{lin.par} = \frac{5Gd^4(r_2^2-r_1^2)}{128\,n_a(r_2^5-r_1^5)} \tag{27}$$

In all cases the stiffness in the linear regime is independent of load but depends on the type of spiral due to different radius distributions. Physically, Eq. (10) also tells us that the linear-regime stiffness is determined by the third moment of the radius distribution along the spring. We conclude that spiral laws affect stiffness not only local properties but also the global radius field.

3.4 Transition to Stacking and Contact Criterion

As load increases, adjacent turns approach one another axially. The onset of stacking occurs when the relative axial deflection between neighboring turns equals the per-turn clearance defined in Eq. (2). The first contact occurs when the deflection between adjacent turns equals the clearance δ_s. From the per-turn contact condition,

$$\frac{64 P r_f^3}{Gd^4} = \delta_s \tag{28}$$

The radius of the last free coil (the free-boundary radius) is:

$$r_f(P) = \left(\frac{Gd^4\delta_s}{64P}\right)^{\frac{1}{3}} \tag{29}$$

Define constant

$$C = \left(\frac{Gd^4\delta_s}{64}\right)^{\frac{1}{3}} \tag{30}$$

where C is a proportionality constant defined by the spring's material and geometric parameters. Therefore

$$r_f(P) = C\,P^{-1/3} \tag{31}$$

This mapping is a central theoretical result. It converts a mechanical loading condition into a geometric boundary condition. Its inverse-cubic structure arises directly from torsional compliance scaling with r^3. Thus, the exponent is not empirical but physically determined.

The transition and full-collapse loads follow as:

$$P_T = \frac{Gd^4\delta_s}{64r_2^3} \tag{32}$$

$$P_C = \frac{Gd^4\delta_s}{64r_1^3} \tag{33}$$

So that stacking occurs in the nonlinear regime $P_T < P < P_C$. These loads define exact regime boundaries without numerical search.

3.5 General Stacking-Regime Deflection Structure

The stacking occurs when the load of transition is exceeded and the spring is in a non-linear regime. The turn domain is divided into two regions: an inner stacked region where the coils touch and only geometrical shortening occurs, and an outer free region where the coils elastically remain active. The total resulting deflection is then the sum of an elastic integral on the free region plus a geometric stacking term proportional to the number of turns in contact:

$$\Delta(P) = \left(n_a - n_f(P)\right)\delta_s + \frac{64\,P}{Gd^4}\int_0^{n_f(P)} r(n)^3\,dn \tag{34}$$

Equation (34) is the universal stacking-regime equation. It applies to any spiral law and preserves analytical continuity because the integration limit is load-dependent but explicit.

3.6 Spiral-Specific Closed-Form Stacking Solutions

For each spiral type, the stacking solution follows a common procedure: invert the spiral law to obtain n(r), evaluate the integral in Eq. (34) up to the boundary radius, and substitute the load–radius mapping from Eq. (31).

From Eq. (3) and Eq. (4), we get

ISSN (online): 2581-3048
Volume 10, Issue 5, pp 304-315, May-2026
https://doi.org/10.47001/IRJIET/2026.105041

$$r_f(n_f) = r_1 + \frac{(r_2 - r_1)}{n_a} n_f \quad (35)$$

Arranging terms and simplifying

$$n_f = \frac{r_f - r_1}{r_2 - r_1} \cdot n_a \quad (36)$$

For the Archimedean spiral, by substituting Eq. (35) and Eq. (36) into Eq. (34) and integrating up to n_f as previously shown,

$$\Delta(P) = \left(n_a - \frac{r_f - r_1}{r_2 - r_1} \cdot n_a\right) \delta_s + \frac{64\,P}{Gd^4} \frac{n_a\left(r_f^4 - r_1^4\right)}{4(r_2 - r_1)} \quad (37)$$

Simplify:

$$\Delta(P) = \left(\frac{r_2 - r_f}{r_2 - r_1}\right) n_a \delta_s + \frac{16 n_a\, P}{Gd^4(r_2 - r_1)}\left(r_f^4 - r_1^4\right) \quad (38)$$

By Substituting Eq. (3.14) into Eq. (3.39) and simplify, we get:

$$\Delta(P) = \frac{r_2 n_a \delta_s}{r_2 - r_1} - \frac{n_a \delta_s C}{r_2 - r_1} P^{-1/3} + \frac{16 n_a C^4}{Gd^4(r_2 - r_1)} P^{-1/3} \frac{16 n_a r_1^4}{Gd^4(r_2 - r_1)} P \quad (39)$$

$$\Delta(P)_{Stacked} = \frac{r_2 n_a \delta_s}{r_2 - r_1} - \frac{n_a \delta_s C}{r_2 - r_1} P^{-1/3}$$

$$\Delta(P)_{\text{Elastic}} = \frac{16 n_a C^4}{Gd^4(r_2 - r_1)} P^{-1/3} - \frac{16 n_a r_1^4}{Gd^4(r_2 - r_1)} P$$

By combine the $P^{-1/3}$ terms from Eq. (30), we get

$$\Delta(P) = \frac{r_2 n_a \delta_s}{r_2 - r_1} - \frac{n_a \delta_s \left(\frac{Gd^4 \delta_s}{64}\right)^{\frac{1}{3}}}{r_2 - r_1} P^{-1/3} + \frac{16 n_a \left(\frac{Gd^4 \delta_s}{64}\right)^{\frac{4}{3}}}{Gd^4(r_2 - r_1)} P^{-1/3} \frac{16 n_a r_1^4}{Gd^4(r_2 - r_1)} P \quad (40)$$

After simplification, we get

$$\Delta_{Arch}(P) = \frac{r_2 n_a \delta_s}{r_2 - r_1} - \frac{3 n_a (Gd^4)^{1/3} {\delta_s}^{4/3}}{16(r_2 - r_1)} P^{-1/3} - \frac{16 n_a r_1^4}{Gd^4(r_2 - r_1)} P \quad (41)$$

Differentiate Equation (41) w.r.t. (P):

$$\frac{d\Delta_{Arch}}{dP} = \frac{1}{3} \cdot \frac{3 n_a (Gd^4)^{1/3} {\delta_s}^{4/3}}{16(r_2 - r_1)} P^{-4/3} - \frac{16 n_a r_1^4}{Gd^4(r_2 - r_1)} \quad (42)$$

Simplify :

$$\frac{d\Delta_{Arch}}{dP} = \frac{n_a (Gd^4)^{1/3} {\delta_s}^{4/3}}{16(r_2 - r_1)} \frac{1}{P^{4/3}} - \frac{16 n_a r_1^4}{Gd^4(r_2 - r_1)} \quad (43)$$

Thus instantaneous stiffness:

$$R_{Arch}(P) = \frac{1}{d\Delta/dP} \quad (44)$$

The structure shows that stacking deflection consists of a cubic boundary-radius term plus a linear geometric stacking term.

From Eq. (5) and Eq. (6), we get

$$n_f = \frac{1}{k} \ln\left(r_f / r_1\right) \quad (45)$$

Equation (45) highlights a key feature of the logarithmic spiral, where the number of remaining elastic turns decreases logarithmically as the stacking process progresses. The total deflection consists of geometric stacking of contacted turns and elastic deformation of free turns.

By substituting Eq. (36) into Eq. (34) and integrating up to n_f, we get:

$$\Delta(P) = \left(n_a - \frac{1}{k} ln \frac{r_f}{r_1}\right) \delta_s + \frac{64\,P}{Gd^4} \cdot \frac{r_f^3}{3k} - \frac{64\,P}{Gd^4} \cdot \frac{r_1^3}{3k} \quad (46)$$

From Eq. (31), we get:

$${r_f}^3 = \frac{C^3}{P} \quad (47)$$

The result of the elastic term in Eq. (46) is extremely significant, since the exponential geometry yields a purely cubic relationship with the free-boundary radius, free of higher-order terms. By Substituting Eq. (31) and Eq. (47) into Eq. (46) and simplify, we get:

$$\Delta_{log}(P) = n_a \delta_s - \frac{\delta_s}{k} ln\, C + \frac{\delta_s}{3k} ln\, P + \frac{\delta_s}{k} ln\, r_1 + \frac{\delta_s}{3k} - \frac{64\,P}{Gd^4} \cdot \frac{r_1^3}{3k} \quad (48)$$

Then

$$\Delta(P)_{\text{Elastic}} = \frac{\delta_s}{3k} - \frac{64\,P}{Gd^4} \cdot \frac{r_1^3}{3k} \quad (49)$$

This exact algebraic cancellation is a defining feature of the logarithmic spiral.

$$\Delta(P)_{Stacked} = n_a \delta_s - \left(\frac{\delta_s}{k} ln\, C - \frac{\delta_s}{3k} ln\, P - \frac{\delta_s}{k} ln\, r_1\right) \quad (50)$$

Differentiate Equation (48) w.r.t. (P):

$$\frac{d\Delta_{log}}{dP} = \frac{\delta_s}{3k} \cdot \frac{1}{P} - \frac{64\, r_1^3}{3kGd^4} \quad (51)$$

Using $P_C = \frac{Gd^4 \delta_s}{64 r_1^3}$, we can write

ISSN (online): 2581-3048
Volume 10, Issue 5, pp 304-315, May-2026
https://doi.org/10.47001/IRJIET/2026.105041

$$\frac{d\Delta_{log}}{dP} = \frac{\delta_s}{3k}\left(\frac{1}{P} - \frac{1}{P_C}\right) \quad (52)$$

Thus stiffness:

$$R_{log}(P) = \frac{1}{\frac{\delta_s}{3k}\left(\frac{1}{P} - \frac{1}{P_C}\right)} \quad (53)$$

The logarithmic spiral stacking formulation is essentially different from the Archimedean case because the radius varies exponentially with the turn index, as defined in Eqs. (5)-(6). This exponential geometry results in a logarithmic relation between the free-boundary radius and the remaining number of elastic turns given by Eq. (45). There is an important mathematical feature in Eqs (48)–(50). Due to the exponential spiral law, higher-order mixed terms cancel exactly, resulting in a compact cubic dependence on the free-boundary radius. This cancellation is unique to the logarithmic spiral and leads to a particularly clean closed-form expression for deflection in the stacking regime. Differentiating the expression for the final deflection with respect to the load (Eq. 51-52) yields the formula for the instantaneous stiffness given in Eq. (53). The stiffness thus changes smoothly with load and reflects the progressive reduction of the active spring region as stacking progresses. For the parabolic spiral, the radius is governed by a quadratic law in turn index (Eq. 7– 9), which leads to a square-root relation when inverted. From ${r_f}^2 = r_1^2 + \beta n_f$

$$n_f = n_a \frac{{r_f}^2 - r_1^2}{{r_2}^2 - r_1^2} \quad (54)$$

Substituting this geometry into the general stacking formulation (Eq. 34) produces the intermediate stacking deflection form

$$\Delta(P) = \left(n_a \frac{r_2^2 - r_f^2}{r_2^2 - r_1^2}\right)\delta_s + \frac{64\,P}{Gd^4}\frac{2n_a}{5(r_2^2 - r_1^2)}\left(r_f^5 - r_1^5\right) \quad (55)$$

Simplify:

$$\Delta(P) = \frac{n_a \delta_s \left(r_2^2 - r_f^2\right)}{r_2^2 - r_1^2} + \frac{128 n_a\, P}{5Gd^4(r_2^2 - r_1^2)}\left(r_f^5 - r_1^5\right) \quad (56)$$

Substitute $r_f(P) = C\,P^{-1/3}$. Evaluate and group terms into constant $P^{-2/3}$ linear-in-P. Using $C^3 = \frac{Gd^4\delta_s}{64}$ and algebraic simplification with $C^5 = C^2C^3$ to remove mixed powers yields the compact final form:

$$\Delta_{par}(P) = \frac{n_a \delta_s r_2^2}{r_2^2 - r_1^2} - \frac{3n_a\left(Gd^4\right)^{2/3}{\delta_s}^{5/3}}{80(r_2^2 - r_1^2)}P^{-2/3} - \frac{128 n_a r_1^5}{5Gd^4(r_2^2 - r_1^2)}P \quad (57)$$

Unlike the logarithmic case, the parabolic spiral gives algebraic powers of mixed degree on substitution. By applying the load–radius relationship in Eq. (31) and the geometric constants in Eq. (8), these mixed terms can be reordered and simplified. The final compact closed-form stacking deflection equation is given in Eq. (57) in terms of a sum of constant, square-root and linear load terms. This structure clearly separates:

- the constant geometric contribution,
- the nonlinear elastic contribution from remaining free coils, and
- the linear stacking contribution proportional to load.

Differentiating Eq. (56) yields

$$\frac{d\Delta_{par}}{dP} = \frac{n_a\left(Gd^4\right)^{2/3}{\delta_s}^{5/3}}{40(r_2^2 - r_1^2)}P^{-5/3} - \frac{128 n_a r_1^5}{5Gd^4(r_2^2 - r_1^2)} \quad (58)$$

The corresponding instantaneous stiffness is can be obtained as

$$R_{par}(P) = \frac{1}{d\Delta/dP} \quad (59)$$

The stiffness variation reflects the quadratic spiral geometry and produces a smooth nonlinear hardening response throughout the stacking regime.

3.7 Continuity, Monotonicity, and Limit Verification

Mathematical consistency of the stacking models is verified through boundary substitution and derivative analysis. Substituting the transition boundary into the stacking equations reduces them exactly to the linear-regime formulas (Eqs. 11–27), proving continuity at P_T. Substituting the collapse boundary eliminates the elastic integral term, reducing deflection to the geometric stacking term alone, consistent with the solid-height condition.

Differentiation of the load–radius mapping yields showing smooth monotonic boundary evolution. Substitution into the differentiated stacking equations (Eqs. 42–43, 51–52) shows that $d\Delta/dP > 0$ throughout the admissible domain, proving monotonic deflection growth. As $P \to P_C$, the elastic contribution vanishes and the slope approaches zero, implying infinite stiffness, a physically correct solid-limit behavior.

3.8 Theoretical Consequences

Because stiffness evolution depends on how rapidly the free-boundary radius shrinks with load, spiral laws with faster radius decay produce faster stiffness growth. From the derived stiffness expressions, a strict ordering follows:

$$k_{\text{logarithmic}} > k_{\text{Archimedean}} > k_{\text{parabolic}}$$

ISSN (online): 2581-3048
Volume 10, Issue 5, pp 304-315, May-2026
https://doi.org/10.47001/IRJIET/2026.105041

This ordering is not empirical but a direct theoretical consequence of radius-growth law structure and the cubic torsional compliance dependence.

IV. MATERIALS AND METHODS

The present study is performed by employing a structured hybrid analytical-computational methodology for the development of a unified closed-form theoretical model for the load-deflection and stiffness behaviour of telescopic conical compression springs defined by continuous spiral radius laws. The modelling framework was designed with a methodological goal of complete reproducibility, in which the geometry, governing mechanics, regime transitions, and response calculations are all explicitly derived from first principles, rather than by empirical fitting or incremental coil summation. Hence, all the work stages from the geometric definition to the evaluation and verification of the response were formulated in analytical form and then evaluated numerically only for the generation of curves and the comparative analysis.The research began with the parametric geometric definition of the spring centreline by using a continuous turn-index representation. Instead of modelling the spring as a collection of discrete coils, the coil centreline radius was modelled as a smooth function of a continuous turn parameter over the active coil domain. To reflect different and mathematically well-defined classes of radius growth, three spiral laws were chosen: Archimedean (linear variation of radius with turn index), logarithmic (exponential variation) and parabolic (quadratic variation). The explicit analytical form of each spiral function was described and constructed to satisfy the same boundary conditions, e.g., inner mean radius, outer mean radius, total number of active turns and wire diameter. By enforcing the same boundary radii and number of turns in all cases, we allow comparison that focuses on the mechanical effect of the spiral growth law itself, as opposed to any global size effects. The spiral relations were also formulated in invertible form, allowing the turn index to be expressed as a function of radius, necessary for derivation of stacking-regime limits and load dependent active domain boundaries. After the geometric definition, the mechanical model was constructed on the basis of the classical theory of closely coiled helical springs. It was assumed that the deformation mechanism was torsion-dominated, that is, the axial deflection under load was mainly due to twisting of the wire rather than bending of the coil centreline. The material was assumed to be linear elastic and isotropic with a constant shear modulus, and the wire cross-section was assumed to be circular and uniform along the length. Other assumptions in the modelling were small pitch angle, quasi-static axial loading and negligible contribution of direct shear and bending curvature. A geometric stacking criterion was used to handle the coil contact during progressive compression. When the axial clearance of the adjacent turns closes without any additional contact compliance or frictional effects, the adjacent turns are removed from elastic participation and stacked. These assumptions are compatible with the well-known analytical spring mechanics and with the torsional compliance framework used in the theoretical development. Provided the above, the load-deflection relation governing this situation was derived from the torsional strain-energy considerations and is given by a continuous compliance integral over the active turn domain. Since the torsional compliance is proportional to the cube of the mean coil radius, the total axial deflection was written as an integral of the radius-cubed field against the turn parameter. This continuous formulation replaces the usual coil-by-coil summation methods and enables an exact analytical evaluation if the radius law is known. In particular, two deformation regimes were studied. The compliance integral is integrated over the entire turn interval, as all turns are elastically active in the linear (all-free) regime. The closed-form linear load-deflection and constant stiffness expressions specific to the spiral The progressive stacking regime proposed a load-dependent boundary radius based on a per-turn clearance condition equating local relative deflection to geometric coil spacing. This condition gives an explicit analytical mapping between the applied load and the radius of the last free coil. Thus, the active domain is truncated analytically, and the total deflection is the addition of an elastic integral over the remaining free turns and a geometric stacking term proportional to the number of contacted turns. From this boundary condition the transition load and the collapse load were obtained directly, giving exact regime limits without numerical search. Closed-form expressions were derived for each spiral law in both regimes and evaluated by symbolic and numerical computation tools. Symbolic processing has been first used to simplify the derived expressions and to reduce them to compact analytical form. Numerical evaluation was done by inserting a compatible set of parameters into all spiral models and calculating response values for a dense load grid over the admissible operating range from zero load to collapse load. Load-deflection curves were directly obtained from analytical equations for each spiral type. Instantaneous stiffness curves were obtained by differentiating the closed-form deflection expressions with respect to load and evaluating the resulting expressions at the same load grid. No numerical fit, regression or curve smoothing was performed; all plotted results are directly derived from the equations obtained. The use of structured post-processing and verification steps ensured correctness and reproducibility. All expressions were checked for dimensional and parameter consistency. The analytical transition load was plugged into the stacking-regime formulas and checked to simplify exactly to the linear-regime deflection formulas, which confirms the regime continuity. The limit was

International Research Journal of Innovations in Engineering and Technology (IRJIET)

ISSN (online): 2581-3048

Volume 10, Issue 5, pp 304-315, May-2026

https://doi.org/10.47001/IRJIET/2026.105041

checked by substituting the collapse load and confirming the elastic integral term disappears and the deflection is only the geometric stacking term as required by the solid-height condition. Monotonicity of the response was checked analytically by analysing the sign of the load derivatives and numerically by checking strictly increasing load-deflection curves. The instantaneous stiffness was compared with numerical slope estimates of the computed curves, obtained from analytical derivatives. Further checks showed that the mapping from load to boundary radius is strictly monotonic and that there are no slope discontinuities at regime transitions. In this way, all the reported curves and comparative results can be directly traced back to the closed-form governing equations obtained by the proposed geometric and mechanical assumptions. In combination, the analytical derivation, parametric evaluation and internal consistency check constitute a transparent and fully reproducible Materials and Methods framework for the spiral-defined telescopic conical spring modelling.

V. RESULTS AND DISCUSSION

In this section, theoretical and computational results obtained from the unified closed-form formulations developed in Section 3 are presented and interpreted. The results section is designed to not only show curves and tables but also to demonstrate how the derived equations explain the nonlinear mechanical behaviour of spiral-defined telescopic conical springs, how the three spiral geometries behave differently, and how regime-based theory is confirmed through internal consistency checks and comparative trends. The figures referred to here are numbered and captioned as they were in the original manuscript file.

5.1 Theoretical Load–Deflection Characteristics

The primary theoretical result of the present model is the full load-deflection relation in the fully free and progressive stacking regimes for the three spiral geometries. Continuous load–deflection curves were generated over the full admissible load range from zero load to collapse load, using the closed-form expressions derived in Section 3, specifically the linear-regime formulas (Eqs. 11–27) and the stacking-regime formulas (Eqs. 41, 48, and 57). The theoretical load-deflection curves of the telescopic conical springs defined by Archimedean, logarithmic and parabolic spiral laws under the same geometric and material parameters are shown in Fig. 1. As all three springs have the same wire diameter, shear modulus, active turns and boundary radii, the differences between the curves are only due to the spiral radius law and its effect on the radius distribution integral and the stacking boundary evolution.

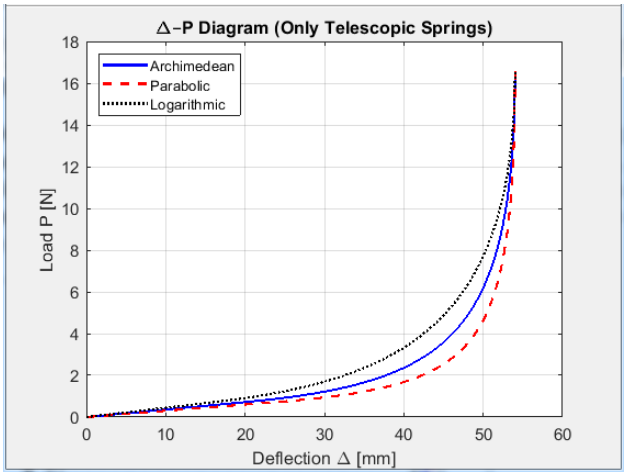

Figure 2: Theoretical load–deflection curves of telescopic conical springs with Archimedean, parabolic, and logarithmic profiles

The load-deflection curves in Figure 1 show a significant nonlinear behaviour, with the load increasing super linearly with the deflection. This behaviour is a direct consequence of the stacking-regime formulation in Eq. (34), where the active elastic domain shrinks with increasing load as the boundary radius decreases as defined by Eq. (31). For small deflections, all the curves collapse on the linear response Eq. (10), with the differences in initial stiffness being determined by the radius-cubed integral. As the load approaches the transition value of Eq. (32), the curves deviate smoothly from linearity, which confirms the analytical continuity between the regimes as shown in Section 3.7 The three spiral geometries exhibit a clear hierarchy in stiffness. For any admissible deflection, the logarithmic spiral carries the greatest load, followed by the Archimedean and the parabolic spiral, as predicted by Eqs. (53) and (59). This ordering follows directly from the different laws of radius-decay and the cubic dependence of the torsional compliance on the radius in Eq. (10). The logarithmic spiral provides a faster response and a faster stiffness amplification, and the smaller radii are focused earlier, while the Archimedean and parabolic spirals generate more and more moderate responses. The transition load is given by Eq. (32) and is the point of coil contact that is manifested as a smooth increase of curvature without any discontinuity in slope or deflection. This confirms the continuity condition proved in Section. 3.7.1, where the stacking expressions reduce exactly to the linear regime at the boundary of transition. Beyond this point the logarithmic spiral displays the fastest nonlinearity, the Archimedean spiral the intermediate response, and the parabolic spiral the slowest evolution. This is in agreement with the boundary sensitivity discussed The lack of slope discontinuities means that regime transitions are analytically embedded, not numerically imposed. The deflection relations (Eqs. 41, 48, 57) in the stacking regime consist of two terms, an elastic term over the remaining active turns and a geometric stacking term proportional to the number of contacted turns.

ISSN (online): 2581-3048
Volume 10, Issue 5, pp 304-315, May-2026
https://doi.org/10.47001/IRJIET/2026.105041

The elastic contribution decreases with the load, and the stacking term increases, leading to a slow increase of the stiffness. The strength of the curvature corresponds with the analytical structure of each formulation, being strongest for the logarithmic spiral (Eq. 48), moderate for the Archimedean (Eq. 41), and least for the parabolic spiral (Eq. 57). In all the cases the derivatives are positive as expected from the conditions obtained in Eqs. (42-43), (51-52) and (58) so that the curves are strictly monotonic.

5.2 Instantaneous Stiffness Evolution

Instantaneous stiffness curves were obtained from the reciprocal slope definition using the derivatives of the stacking equations in closed form. The evolution of the stiffness can be readily obtained from Eqs. (44), (53) and (59). The stiffness increases monotonically with load in the stacking regime for all spiral types in agreement with the theoretical prediction of progressive loss of active turns and continuous reduction of compliance. The slope of the load-deflection curve approaches zero, and the instantaneous stiffness diverges at the load of collapse given by Eq. (33). This asymptotic behaviour can be observed in the high load tail of the calculated curves and is in accordance with the limit analysis presented in Section 3.7 Physically, this is the approach to solid height. Small additional deflection due to additional load. The comparative stiffness plots (the same as the stiffness figures in the original file) show that the logarithmic spiral has the largest stiffness in the stacking regime, followed by the Archimedean and parabolic. The spacing between stiffness curves grows with load. This means that the spiral law dominates more deeply in the stacking regime than in the linear regime.

5.3 Numerical Value Comparison at Representative Deflections

Table 1 further illustrates the stiffness hierarchy of the representative numerical values reported. The predicted load of the logarithmic spiral is higher than that of the Archimedean spiral at each deflection level shown, which is higher than that of the parabolic spiral. The differences grow with deflection, confirming the nonlinearity of the spiral-law influence and its increase with the stacking progression, rather than its constancy.

Table 1: The stiffness hierarchy

Deflection (mm)	Logarithmic (N)	Archimedean (N)	Parabolic (N)
10	0.446	0.360	0.301
20	0.910	0.719	0.603
30	1.697	1.220	0.941
40	3.329	2.362	1.680
50	7.713	6.193	4.638

This behavior is consistent with the theory because the boundary-radius mapping in Eq. (31) introduces a nonlinear coupling between load and active radius domain. Spiral laws with faster radius contraction produce faster domain contraction and therefore stronger stiffness amplification at higher loads.

5.4 Consistency Checks and Model Self-Verification

The derived formulas and the computed curves have been internally checked for consistency several times. First, substituting the transition load into the stacking equations reproduced the linear-regime deflection values to numerical precision, confirming analytical continuity. Secondly, the substitution of the collapse load resulted in deflections equal to the telescopic solid height prediction, confirming correct collapse limits. Thirdly, numerical differentiation of the computed curves agreed with the analytical stiffness formulas and thus confirmed the correctness of the derivative. Residual checks of the load–radius mapping indicated a monotonically decreasing boundary radius with load as predicted .No regime reversals or non-physical oscillations were observed. These checks show the consistency and numerical stability of the theoretical framework throughout the whole domain.

5.5 Design Interpretation of Results

From a design perspective, the results demonstrate that spiral-law selection provides a straightforward and predictable approach to customising nonlinear stiffness. Logarithmic spirals are more suitable for applications with fast growth in stiffness and high load capacity at moderate deflections. Archimedean spirals show well-balanced, non-linear behaviour with a moderate progression. Parabolic spirals provide for smoother compliance and a larger low-stiffness range before rapid hardening. These conclusions are derived directly from closed-form equations and not from fitted curves, and they are therefore amenable to use in parametric design and optimisation workflows. The results thus confirm not only the correctness of the theory, but also its practical utility in design.

REFERENCES

[1] Wahl, A. M. (1963). Mechanical springs (2nd ed.). McGraw-Hill.
[2] Shigley, J. E., & Mischke, C. R. (2015). Mechanical engineering design (10th ed.). McGraw-Hill Education.
[3] Paredes, M., &Daidie, A. (2010). Optimal catalogue selection and custom design of Belleville spring arrangements. International Journal of Interactive Design and Manufacturing, 4(1), 51–59. https://doi.org/10.1007/s12008-009-0086-4

ISSN (online): 2581-3048
Volume 10, Issue 5, pp 304-315, May-2026
https://doi.org/10.47001/IRJIET/2026.105041

[4] Institute of Spring Technology. (2005). Essential spring design training course handbook. Sheffield, United Kingdom.

[5] Dym, C. L. (2009). Consistent derivations of spring rates for helical springs. Journal of Mechanical Design, 131, 031001. https://doi.org/10.1115/1.3125888

[6] Ding, X., & Selig, J. M. (2004). On the compliance of coiled springs. International Journal of Mechanical Sciences, 46, 703–727. https://doi.org/10.1016/j.ijmecsci.2004.05.009

[7] SAE International. (2019). SAE spring design manual. SAE International.

[8] Tahir, M. S. A.-D., Hassan, S. S., & Chiad, J. S. (2022). The mathematical model for lateral stiffness of variable length conical spring. International Review of Applied Sciences and Engineering, 13(1), 31–35. https://doi.org/10.1556/606.2021.00494

[9] Paredes, M., &Daidie, A. (2010). Optimal catalogue selection and custom design of Belleville spring arrangements. International Journal of Interactive Design and Manufacturing, 4(1), 51–59. https://doi.org/10.1007/s12008-009-0086-4

[10] Paredes, M., Sartor, M., &Masclet, C. (2002). Obtaining an optimal compression spring design directly from a user specification. Proceedings of the Institution of Mechanical Engineers, Part B: Journal of Engineering Manufacture, 216, 419–428. https://hal.science/hal-03744438v1

[11] Jiang, W. G., & Henshall, J. L. (2000). A novel finite element model for helical springs. Finite Elements in Analysis and Design, 35, 363–377. https://doi.org/10.1016/S0168-874X(99)00076-1

[12] Chassie, G. G., Becker, L. E., & Cleghorn, W. L. (1997). On the buckling of helical springs under combined compression and torsion. International Journal of Mechanical Sciences, 39(6), 697–704. https://doi.org/10.1016/S0020-7403(96)00070-7

[13] Becker, L. E., Chassie, G. G., & Cleghorn, W. L. (2002). On the natural frequencies of helical compression springs. International Journal of Mechanical Sciences, 44, 825–841. https://doi.org/10.1016/S0020-7403(01)00096-0

[14] Todinov, M. T. (1999). Maximum principal tensile stress and fatigue crack origin for compression springs. International Journal of Mechanical Sciences, 41, 357–370. https://doi.org/10.1016/S0020-7403(98)00068-X

[15] Wu, M. H., & Hsu, W. Y. (1998). Modelling the static and dynamic behavior of a conical spring by considering coil close and damping effects. Journal of Sound and Vibration, 214(1), 17–28. https://doi.org/10.1006/jsvi.1997.1511

[16] Paredes, M., Sartor, M., &Masclet, C. (2002). Obtaining an optimal compression spring design directly from a user specification. Proceedings of the Institution of Mechanical Engineers, Part B: Journal of Engineering Manufacture, 216, 419–428. https://hal.science/hal-03744438v1

[17] Qiu, D., Seguy, S., & Paredes, M. (2018). Tuned nonlinear energy sink with conical spring: Design theory and sensitivity analysis. Journal of Mechanical Design, 140(1), 011404. https://doi.org/10.1115/1.4038304

[18] Patel, H., & Zhou, H. (2021). Analysis and synthesis of conical coil springs. ASME International Design Engineering Technical Conferences, Paper No. DETC2021-69971. https://doi.org/10.1115/DETC2021-69971

[19] Mishra, A., & Aggarwal, M. L. (2020). Comparative deflection analysis of conical compression spring with standard constant rate helical spring. IOP Conference Series: Materials Science and Engineering, 804, 012010. https://doi.org/10.1088/1757-899X/804/1/012010W

Citation of this Article:

Ali Khayoun Al-Janabi, & Essam L. Esmail. (2026). Unified Closed-Form Load–Deflection Modeling of Spiral-Defined Telescopic Conical Compression Springs. *International Research Journal of Innovations in Engineering and Technology - IRJIET*, 10(5), 304-315. Article DOI https://doi.org/10.47001/IRJIET/2026.105041

****

